Physica A 388 (2009) 2535–2546

Contents lists available at ScienceDirect

Physica A

journal homepage: www.elsevier.com/locate/physa

Imperfect targeted immunization in scale-free networks

Yubo Wang [a], Gaoxi Xiao [a,*], Jie Hu [a], Tee Hiang Cheng [a], Limsoon Wang [b,c]

[a] School of Electrical and Electronic Engineering, Nanyang Technological University, Singapore 639798, Singapore
[b] School of Computing, National University of Singapore, Singapore 117543, Singapore
[c] School of Medicine, National University of Singapore, Singapore 117543, Singapore

ARTICLE INFO

Article history:
Received 3 October 2008
Received in revised form 24 January 2009
Available online 5 March 2009

PACS:
89.75.-k
89.75.Fb
05.70.Ln

Keywords:
Scale-free network
Imperfect immunization
Epidemic threshold
Average outbreak size
Degree-correlated SIR

ABSTRACT

Scale-free networks are prone to epidemic spreading. To provide cost-effective protection for such networks, targeted immunization was proposed to selectively immunize the hub nodes. In many real-life applications, however, the targeted immunization may not be perfect, either because some hub nodes are hidden and consequently not immunized, or because the vaccination simply cannot provide perfect protection. We investigate the effects of imperfect targeted immunization in scale-free networks. Analysis and simulation results show that there exists a linear relationship between the inverse of the epidemic threshold and the effectiveness of targeted immunization. Therefore, the probability of epidemic outbreak cannot be significantly lowered unless the protection is reasonably strong. On the other hand, even a relatively weak protection over the hub nodes significantly decreases the number of network nodes ever getting infected and therefore enhances network robustness against virus. We show that the above conclusions remain valid where there exists a negative correlation between nodal degree and infectiousness.

1. Introduction

Many real-life complex systems can be described as networks [1,2]. The well-known examples include the Internet [3], World-Wide Web (WWW) [4], food web [5–7], and the human society [8]. Studies on these systems as networks have spawned a new research area called complex networks [2,9]. Statistical studies on real-life complex networks show that though different systems have different features [2], many of them share some nontrivial features. One of the most noticeable features is that a large number of them turn out to be scale-free networks of which the nodal degrees follow a power-law distribution. Specifically, the probability that a node is connected to k other nodes is

$$P(k) \sim k^{-r}, \tag{1}$$

where the exponent r usually ranges between 2 and 3 [2]. In a scale-free network, a large number of nodes have low degrees while a small number of nodes have very high degrees. It is known that scale-free networks enable efficient communications but they are prone to disease/virus spreading [10,11].

Studies on epidemic spreading are strongly motivated by the threats we are facing, e.g., virus spreading in the Internet [11] and infectious diseases such as HIV in human society [8]. Within networks, virus lives and proliferates in network nodes and propagates via links. Recent research shows that epidemic spreading in an infinitely large scale-free network with an exponent $r \leq 3$ does not possess any epidemic threshold below which the infection cannot produce a major epidemic outbreak or an endemic state [11–14]. In other words, statistically speaking, a virus can easily survive and

* Corresponding author. Tel.: +65 6790 4552; fax: +65 6793 3318.
E-mail address: egxxiao@ntu.edu.sg (G. Xiao).

0378-4371/$ – see front matter
doi:10.1016/j.physa.2009.02.036

cause an outbreak in an infinitely large scale-free network no matter how weak its spreading capability is. Further studies on the finite-size scale-free networks show that the epidemic threshold remains to be low and decreases with an increasing network size [15]. Such analytical results help to explain our real-life experiences, e.g., persistent virus spreading in the Internet.

Due to the peculiar connection pattern in scale-free networks, a small number of nodes have very high degrees. The random immunization strategy is not effective in preventing an epidemic outbreak or reducing the number of infections in a scale-free network though such a strategy works very well in homogeneous random networks [16,17]. New immunization strategies have to be developed to recover the epidemic threshold. One of the most efficient approaches is to immunize those nodes with the highest degrees, or, more specifically, to immunize those nodes (hereafter termed as hubs or hub nodes) with degrees higher than a preset cut-off value k_c. Such a strategy is known as targeted immunization [16].

In existing studies on targeted immunization, it is generally assumed that all hub nodes are immunized; and once a hub is immunized, it will never be infected. We realize that in many real-life systems, this may not always be the case, either because the immunizations have missed some hubs or because the vaccination is not 100% effective [18–21]. In this paper, we consider three different cases as follows:

(i) Some hub nodes may be hidden and hence not immunized. This is more likely to happen in large-scale systems. We term this case *Partial Node Immunization* (PNI);
(ii) The vaccination cannot provide 100% protection over the immunized nodes but can lower their chance of getting infected. We call this case *Partial Effective Immunization* (PEI);
(iii) The vaccination cannot stop disease propagation through some network links. In other words, an immunized hub may still be infected by some, though not all, of its adjacent nodes. This may happen between family members or trusted partners, etc. We call it *Partial Link Immunization* (PLI).

For all the three different cases, we introduce the immunization rate a. Specifically, in PNI, it denotes the percentage of the hubs that are (perfectly) immunized; in PEI, it denotes the effectiveness of vaccination. In other words, each immunized hub has a probability of $1 - a$ to act as a susceptible node; and in PLI, it denotes the percentage of protected links connected to the hub nodes.

Based on the Susceptible-Infected-Removed (SIR) model [22,23], we analyze the epidemic threshold and the portion of network nodes ever got infected until the disease dies out (hereafter termed as Average Outbreak Size (AOS)) for these three different cases in scale-free networks. We find that there is a linear relationship between the inverse of the epidemic threshold and the immunization rate; therefore, only a high immunization rate can significantly increase the epidemic threshold. However, even a relative low immunization rate can still greatly reduce AOS; the network robustness against epidemic spreading is therefore enhanced. We show that such conclusions remain valid where there exists a negative correlation between nodal degree and infectiousness (i.e., a higher-degree node has a lower chance to pass the disease to each of its adjacent nodes).

2. Models

2.1. Susceptible-Infected-Removed (SIR) model

In this paper, due to page limit, we consider only the SIR model. Study results based on susceptible-infected-susceptible (SIS) model [21,22] are briefly summarized in Section 5, while further details have to be presented in a separate report.

The original SIR model was proposed (though never published) by Reed and Frost in 1920s. In SIR, network nodes are divided into three groups: Susceptible (S), Infected (I), and Removed (R). Susceptible nodes are free of disease but can be infected via direct contacts with infected nodes. Infected nodes carry the disease and can pass it to susceptible nodes. Removed nodes have either recovered from the disease or died; in either case, they cannot pass the disease to other nodes or be infected again. In the classic SIR model, time is slotted. In each time slot, a susceptible node becomes infected at a rate of λ ($\lambda \leq 1$) if it is directly connected to at least one infected node [10,13]. The parameter λ is the microscopic spreading rate (also known as the infection rate). Meanwhile, an infected node becomes a removed node at the rate of δ ($\delta \leq 1$). Without loss of generality, throughout this paper we set $\delta = 1$ [10,13].

Recent studies considered the case where there exists a negative correlation between nodal degree and infectiousness [24–26]. In other words, a higher-degree node may have a lower chance to admit the disease from or pass the disease to each of its adjacent nodes. Such models probably better resemble some real-life cases, e.g., the transmission of sexual diseases [25]. In this paper, we adopt the simple yet rather general model in Ref. [24] that a k-degree infected node spreads the disease to each of its adjacent nodes at a possibility of $T(k)$; and a k'-degree susceptible node admits an infection at a rate of $\lambda'(k') = \lambda A(k')$ if it is connected to at least one infected node. $T(k)$ and $A(k)$ are the correlation functions. To differentiate from the classic SIR model, we term such an extended model as *degree-correlated SIR model*.

Unless otherwise specified, in this paper we study the effects of imperfect targeted immunizations in the classic SIR model. The main conclusions however remain valid for the degree-correlated SIR model, as we shall see in Sections 3.4 and 4.3. As mentioned earlier, two metrics will be adopted in the evaluations: (i) epidemic threshold λ_c, which is a critical spreading rate below which infections die out exponentially and above which an epidemic outbreak will happen; and (ii) AOS.

2.2. Imperfect Targeted Immunization

In the classic targeted immunization, vaccinations are deployed to all hub nodes with degrees greater than k_c while non-hub nodes are not immunized. In PNI with an immunization rate of a, a fraction a of the hub nodes are randomly selected to be perfectly immunized while the others are not immunized. In PEI, a hub node is infected at a rate of $(1-a)\lambda$ if it is directly connected to at least one infected node. In PLI, immunized hub nodes can be infected at a rate of λ by a fraction $1-a$ of its randomly selected adjacent nodes but never by the rest of the adjacent nodes.

In all the three different cases, a non-hub node can be infected at a rate of λ if it is directly connected to at least one infected node; and the infected nodes are removed at a unity rate. Apparently $a = 1$ corresponds to the case of the classic perfect targeted immunization and $a = 0$ corresponds to the case of no immunization.

2.3. Network models

The simulation results presented in this paper are based on two different network models: Barabási–Albert (BA) model [2,27,28] and Autonomous System (AS) level Internet model [29].

The BA model incorporates two important general concepts: growth and preferential attachment. It is an uncorrelated network for which the probability that any two nodes are directly connected is proportional to the product of their nodal degrees.

The AS-level Internet model comes from the real-life data collected in the National Laboratory for Applied Network Research (NLANR) project on January 2, 2000, which contains 6474 nodes connected by 12,572 links. It has been verified that this model closely resembles a scale-free network. It is a disassortative network [30] in which high-degree nodes tend to connect to low-degree nodes.

3. Theoretical analysis

We perform theoretical analysis on the uncorrelated scale-free network model (e.g., the BA model). Analysis on correlated network models is notoriously complicated [12–16] and thus has to be left out for a separate report. We argue that the analysis on the uncorrelated network model, simple as it is, can nevertheless reveal some properties that are valid in many other networks, as has been observed in a few existing studies [10,13,15,16,31,32]. In this paper, our theoretical analyses focus on studying the epidemic threshold and AOS.

3.1. Partial Node Immunization (PNI)

Denote the densities of infected, susceptible, removed and immunized nodes with degree k at time t as $S_k(t)$, $\rho_k(t)$, $R_k(t)$ and $I_k(t)$, respectively. We have

$$S_k(t) + \rho_k(t) + R_k(t) + I_k(t) = 1. \tag{2}$$

Following Moreno, Pastor-Satorras and Vespignani et al. [13,16], by applying the dynamical mean-field (MF) theory [33], PNI can be described by the following differential equations:

$$\frac{\mathrm{d}\rho_k(t)}{\mathrm{d}t} = -\rho_k(t) + \lambda k S_k(t)\theta(t); \tag{3}$$

$$\frac{\mathrm{d}S_k(t)}{\mathrm{d}t} = -\lambda k S_k(t)\theta(t); \tag{4}$$

$$\frac{\mathrm{d}R_k(t)}{\mathrm{d}t} = \rho_k(t), \tag{5}$$

where $\theta(t)$ denotes the probability that a randomly selected link is connected to an infected node at time t. The term $\lambda k S_k(t)\theta(t)$ in Eqs. (3) and (4) indicates the percentages of k-degree nodes which are newly infected. It is a reasonable approximation to the general expression $\lambda S_k(t)\{1-[1-\theta(t)]^k\}$ at a low spreading rate: where a small number of nodes are infected at a close-to-threshold spreading rate, the density of the infected nodes $\rho_k(t)$ approaches zero; hence $\theta(t) \ll 1$.

For any uncorrelated network, the probability that a randomly selected link points to a k-degree node is proportional to $kP(k)$ [10,30]. Therefore in PNI,

$$\theta(t) = \frac{\sum_k kP(k)\rho_k(t)}{\sum_s sP(s)} = \frac{\sum_k kP(k)\rho_k(t)}{\langle k\rangle}, \tag{6}$$

where $\langle k\rangle$ denotes the average nodal degree. Assume that at the beginning of epidemic spreading only a very small fraction of nodes are infected and randomly distributed within the network; or in other words, $\rho_k(0) \doteq 0$. Since in PNI the density

of the immunized nodes is $I_k(t) = a$ for $k > k_c$ and $I_k(t) = 0$ otherwise, the initial conditions can be stated as:

$$\begin{cases} \rho_k(0) = 0, & R_k(0) = 0, & S_k(0) = 1 - a, & I_k(t) = a & \text{if } k > k_c, \\ \rho_k(0) = 0, & R_k(0) = 0, & S_k(0) = 1, & I_k(t) = 0 & \text{if } k \le k_c. \end{cases} \tag{7}$$

Considering Eq. (4) with the initial conditions as in Eq. (7), we derive the density of the susceptible nodes as

$$S_k(t) = \begin{cases} e^{-\lambda k \int_0^t \theta(t')dt' + \ln(1-a)} & \text{if } k > k_c, \\ e^{-\lambda k \int_0^t \theta(t')dt'} & \text{if } k \le k_c. \end{cases} \tag{8}$$

Defining an auxiliary function $\phi(t)$ as representing the value of integration in the exponent in Eq. (8) and replacing $\theta(t)$ by Eq. (6), we have

$$\begin{aligned} \phi(t) &= \int_0^t \theta(t')dt' = \int_0^t \frac{\sum_k kP(k)\rho_k(t')}{\langle k\rangle} dt^t = \frac{\sum_k kP(k)\int_0^t \rho_k(t')dt'}{\langle k\rangle} \\ &= \frac{1}{\langle k\rangle}\sum_k kP(k)R_k(t). \end{aligned} \tag{9}$$

From Eq. (9), we see that $\phi(t)$ actually represents the probability that a randomly selected link points to a removed node at time t. Taking differentiation of $\phi(t)$, we have a self-consistent equation of $\phi(t)$ that

$$\begin{aligned} \frac{d\phi(t)}{dt} &= \frac{1}{\langle k\rangle}\sum_k kP(k)\rho_k(t) = \frac{1}{\langle k\rangle}\sum_k kP(k)[1 - R_k(t) - S_k(t) - I_k(t)] \\ &= 1 - \frac{1}{\langle k\rangle}\sum_{k_{c+1}}^{k_u} kP(k)I_k(t) - \phi(t) - \frac{1}{\langle k\rangle}\sum_k kP(k)S_k(t). \end{aligned} \tag{10}$$

Here k_t and k_u denote the minimum and maximum nodal degrees of the network respectively, and $k_{c+1} = k_c + 1$. At the steady state of epidemic spreading where $t \to \infty$ and $\lim_{t\to\infty} \frac{d\phi(t)}{dt} = 0$, we can derive from Eq. (10) that

$$\begin{aligned} \phi(\infty) &= 1 - \frac{1}{\langle k\rangle}\sum_{k_{c+1}}^{k_u} kP(k)I_k(\infty) - \frac{1}{\langle k\rangle}\sum_k kP(k)S_k(\infty) \\ &= 1 - \frac{1}{\langle k\rangle}\sum_{k_{c+1}}^{k_u} kP(k)I_k(\infty) - \frac{1}{\langle k\rangle}\left[\sum_{k_t}^{k_c} kP(k)e^{-\lambda k\phi(\infty)} + \sum_{k_{c+1}}^{k_u} kP(k)e^{-\lambda k\phi(\infty)+b}\right] \\ &= F(\phi(\infty)). \end{aligned} \tag{11}$$

Obviously $\phi(\infty) = 0$ is a solution of Eq. (11), corresponding to the case where there is no epidemic outbreak. To have an epidemic outbreak, there must be a non-zero solution of $\phi(\infty)$ in the interval $(0, 1 - \frac{1}{\langle k\rangle}\sum_{k_{c+1}}^{k_u} kP(k)I_k(t))$ satisfying

$$\left.\frac{dF(\phi(\infty))}{d\phi(\infty)}\right|_{\phi(\infty)=0} > 1, \tag{12}$$

which defines the epidemics threshold λ_c for PNI as [11,14]

$$\lambda_c^{-1} = \frac{1}{\langle k\rangle}\left[\sum_{k_t}^{k_u} k^2P(k) - a\sum_{k_{c+1}}^{k_u} k^2p(k)\right]. \tag{13}$$

Eq. (13) applies to any uncorrelated network with degree distribution $P(k)$. For an N-node BA model where $P(k) = 2m^2/k^3$, $\langle k\rangle = 2m$ and $k_u \doteq mN^{1/2}$ [27,34], applying the continuum theory to Eq. (13), we have the expression of epidemic threshold that

$$\lambda_c^{-1} = \frac{1}{2}m\ln N - am\ln\frac{mN^{1/2}}{k_{c+1}}. \tag{14}$$

Eqs. (13) and (14) show that there is a linear relationship between the inverse epidemic threshold λ_c^{-1} and the immunization rate a. Hence the epidemic threshold cannot be significantly increased unless the immunization protection is reasonably strong. Fig. 1 shows the dependence of epidemic threshold on the immunization rate and the cut-off. It is also clear that in infinitely large scale-free networks, the epidemic threshold would remain close to zero even when only a small portion of hub nodes are not very well protected.

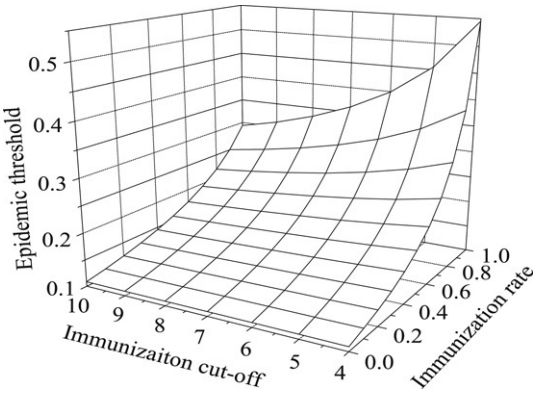

Fig. 1. Dependence of epidemic threshold on immunization rate and immunization cut-off in the BA model.

Note that for the special cases where $a = 0$ and 1, Eqs. (13) and (14) correspond to the well-known cases with no immunization [13] and perfect targeted immunization [16] respectively. By setting $k_c = k_t$, Eqs. (13) and (14) describe the case with global random immunization [16,17].

Denote R_∞ as the network AOS. By adopting the continuum theory, we have

$$\begin{aligned} R_\infty &= 1 - \sum_k P(k) I_k(\infty) - \sum_k P(k) S_k(\infty) \\ &= 1 - \frac{am^2}{k_{c+1}^2} - \left[\sum_{k_t}^{k_{c+1}} \frac{2m^2}{k^3} \mathrm{e}^{-\lambda k \phi(\infty)} + (1-a) \sum_{k_{c+1}}^{k_u} \frac{2m^2}{k^3} \mathrm{e}^{-\lambda k \phi(\infty)} \right] \\ &\doteq 1 - \frac{am^2}{k_{c+1}^2} - \left(\int_{k_t}^{\infty} \frac{2m^2}{k^3} \mathrm{e}^{-\lambda k \phi(\infty)} \mathrm{d}k - a \int_{k_{c+1}}^{\infty} \frac{2m^2}{k^3} \mathrm{e}^{-\lambda k \phi(\infty)} \mathrm{d}k \right). \end{aligned} \tag{15}$$

In the above equation, we assume that k_u is of a very large or infinite value, which is a reasonable approximation in ultra-large scale-free networks [28,29]. Denote $z_1 = \lambda k_t \phi(\infty)$ and $z_2 = \lambda k_{c+1} \phi(\infty)$. For a spreading rate close to the epidemic threshold, we have $z_1 \to 0$, and $z_2 \to 0$. Therefore, Eq. (15) can be re-written as

$$R_\infty = 1 - \frac{am^2}{k_{c+1}^2} - 2m^2 \left(\frac{z_1^2}{k_t^2} \int_{z_1}^{\infty} x^{-3} \mathrm{e}^{-x} \mathrm{d}x - a \frac{z_2^2}{k_{c+1}^2} \int_{z_2}^{\infty} x^{-3} \mathrm{e}^{-x} \mathrm{d}x \right). \tag{16}$$

The integrations in Eq. (16) are in the form of incomplete gamma function $\Gamma(a, z) = \int_z^\infty t^{a-1} \mathrm{e}^{-t} \mathrm{d}t$ with the property that for $z \to 0$,

$$\Gamma(a+1, z) = a\Gamma(a, z) + z^a \mathrm{e}^{-z}, \tag{17}$$

$$\Gamma(0, z) \doteq -r_E - \ln(z) + z + o(z^2), \tag{18}$$

where r_E is the Euler constant [35]. By neglecting the higher-order terms in Eqs. (16)–(18), Eq. (16) can be expressed as

$$\begin{aligned} R_\infty &= 1 - \frac{am^2}{k_{c+1}^2} - 2m^2 \left[\frac{1}{k_t^2} \left(\frac{1}{2} - z_1 \right) - a \frac{1}{k_{c+1}^2} \left(\frac{1}{2} - z_2 \right) \right] \\ &= m\lambda\phi(\infty) \left(2 - \frac{am}{k_{c+1}} \right). \end{aligned} \tag{19}$$

The only unknown term in Eq. (19) is $\phi(\infty)$. From the self-consistent Eq. (11), we have

$$\begin{aligned} \phi(\infty) &= 1 - \frac{1}{\langle k \rangle} \sum_{k_{c+1}}^{k_u} k P(k) I_k(t) - \frac{1}{\langle k \rangle} \sum_k k P(k) S_k(\infty) \\ &= 1 - \frac{ma}{k_{c+1}} - m \left(\int_{k_t}^{k_u} k^{-2} \mathrm{e}^{-\lambda k \phi(\infty)} \mathrm{d}k - a \int_{k_{c+1}}^{k_u} k^{-2} \mathrm{e}^{-\lambda k \phi(\infty)} \mathrm{d}k \right). \end{aligned} \tag{20}$$

The integrations are again in the form of incomplete gamma function. Let $z_1 = \lambda k_t \phi(\infty)$ and $z_2 = \lambda k_{c+1} \phi(\infty)$. Eq. (20) can be re-written as:

$$\phi(\infty) = 1 - \frac{ma}{k_{c+1}} - m \left(\frac{z_1}{k_t} \int_{z_1}^{\infty} x^{-2} \mathrm{e}^{-x} \mathrm{d}x - a \frac{z_2}{k_{c+1}} \int_{z_2}^{\infty} x^{-2} \mathrm{e}^{-x} \mathrm{d}x \right). \tag{21}$$

Applying the properties of the incomplete gamma function and its expansion as shown in Eqs. (17) and (18), we have

$$\phi(\infty) = z_1 - r_E z_1 - z_1 \ln z_1 - \frac{ma}{k_{c+1}} z_2 + \frac{ma}{k_{c+1}} r_E z_2 + \frac{ma}{k_{c+1}} z_2 \ln z_2. \tag{22}$$

Replacing z_1 and z_2 by their respective expressions, we have

$$A\phi(\infty) + B\phi(\infty)\ln\phi(\infty) = 0, \tag{23}$$

where $A = [1-(1-a)\lambda m + (1-a)r_E\lambda m + \lambda m \ln(\lambda m) - a\lambda m \ln(\lambda k_{c+1})]$ and $B = (1-a)\lambda m$. Hence $\phi(\infty)$ can be calculated as

$$\phi(\infty) = \exp\left(-\frac{A}{B}\right). \tag{24}$$

Combining Eqs. (19) and (24), we can predict the network AOS as a function of immunization rate, spreading rate and immunization cut-off for an infinite-size scale-free network. For finite-size networks, the analytical result reflects the trend of AOS changes in PNI as long as the network is large enough.

3.2. Partially Effective Immunization (PEI)

The same set of symbols has been adopted in the analysis of PEI. Still by applying the dynamical mean-field theory, we describe PEI by the following set of coupled differential equations:

$$\frac{\mathrm{d}\rho_k(t)}{\mathrm{d}t} = \begin{cases} -\rho_k(t) + (1-a)\lambda k S_k(t)\theta(t) & \text{if } k > k_c, \\ -\rho_k(t) + \lambda k S_k(t)\theta(t) & \text{if } k \le k_c; \end{cases} \tag{25}$$

$$\frac{\mathrm{d}S_k(t)}{\mathrm{d}t} = \begin{cases} -(1-a)\lambda k S_k(t)\theta(t) & \text{if } k > k_c, \\ -\lambda k S_k(t)\theta(t) & \text{if } k \le k_c; \end{cases} \tag{26}$$

$$\frac{\mathrm{d}R_k(t)}{\mathrm{d}t} = \rho_k(t). \tag{27}$$

Eqs. (25)–(27) are valid in evaluating the onset of infections close to the epidemic threshold where $\rho_k(t) \ll 1$ and $\theta(t) \ll 1$. Similarly to that in Eqs. (3) and (4), $(1-a)\lambda S_k(t)\{1-[1-\theta(t)]^k\}$ is replaced by $(1-a)\lambda k S_k(t)\theta(t)$. The probability that a randomly selected link is connected to an infected node can still be expressed as

$$\theta(t) = \frac{\sum_k kP(k)\rho_k(t)}{\langle k\rangle}. \tag{28}$$

Still assume the initial condition as $R_k(0) = 0$, $\rho_k(t) \doteq 0$, and $S_k(0) = 1 - \rho_k(0) \doteq 1$. We have

$$S_k(t) = \begin{cases} \mathrm{e}^{-(1-a)\lambda k \int_0^t \theta(u)\mathrm{d}u} & \text{if } k > k_c\ , \\ \mathrm{e}^{-\lambda k \int_0^t \theta(u)\mathrm{d}u} & \text{if } k \le k_c. \end{cases} \tag{29}$$

Define an auxiliary function $\phi(t) = \int_0^t \theta(u)\mathrm{d}u$,

$$\begin{aligned} \phi(t) &= \frac{1}{\langle k\rangle}\int_0^t \sum_k kP(k)\rho_k(u)\mathrm{d}u = \frac{1}{\langle k\rangle}\sum_k kP(k)\int_0^t \rho_k(u)\mathrm{d}u \\ &= \frac{1}{\langle k\rangle}\sum_k kP(k)R_k(t). \end{aligned} \tag{30}$$

Taking differentiation of $\phi(t)$, we have the self-consistent equation of $\phi(t)$ where

$$\begin{aligned} \frac{\mathrm{d}\phi(t)}{\mathrm{d}t} &= \frac{1}{\langle k\rangle}\sum_k kP(k)\rho_k(t) = \frac{1}{\langle k\rangle}\sum_k kP(k)[1 - R_k(t) - S_k(t)] \\ &= 1 - \phi(t) - \frac{1}{\langle k\rangle}\sum_k kP(k)S_k(t). \end{aligned} \tag{31}$$

At the steady state where $t \to \infty$, all the infected nodes are removed. Therefore we have $\rho_k(\infty) = 0$ and $\lim_{t\to\infty}\frac{\mathrm{d}\phi(t)}{\mathrm{d}t} = 0$. From Eq. (31), we obtain $\phi(t)$ as

$$\phi(\infty) = 1 - \frac{1}{\langle k\rangle}\sum_k kP(k)S_k(\infty). \tag{32}$$

From Eqs. (28) and (32), we have

$$\phi(\infty) = 1 - \frac{1}{\langle k\rangle}\left[\sum_{k_c+1}^{k_u} kP(k)\mathrm{e}^{-(1-a)\lambda k\phi(\infty)} + \sum_{k_t}^{k_c} kP(k)\mathrm{e}^{-\lambda k\phi(\infty)}\right]. \tag{33}$$

Similarly to the case of PNI, we define an auxiliary function

$$F(\phi(\infty)) = 1 - \frac{1}{\langle k\rangle}\left[\sum_{k_c+1}^{k_u} kP(k)\mathrm{e}^{-(1-a)\lambda k\phi(\infty)} + \sum_{k_t}^{k_c} kP(k)\mathrm{e}^{-\lambda k\phi(\infty)}\right]. \tag{34}$$

To ensure that $\phi(\infty) = F(\phi(\infty))$ has a non-zero root between 0 and 1, subject to the constraint that $\phi(\infty) = 0$ is a solution of this equation, the following condition has to be satisfied [13,16]:

$$\left.\frac{\mathrm{d}F(\phi(\infty))}{\mathrm{d}\phi(\infty)}\right|_{\phi(\infty)=0} > 1. \tag{35}$$

Therefore,

$$\frac{1}{\langle k\rangle}\left[\sum_{k_c+1}^{k_u} kP(k)(1-a)\lambda k + \sum_{k_t}^{k_c} kP(k)\lambda k\right] > 1. \tag{36}$$

Similar to Eq. (10), Eq. (34) defines the epidemic threshold, which can be calculated as

$$\lambda_c^{-1} = \frac{1}{\langle k\rangle}\left[\sum_{k_t}^{k_u} k^2P(k) - a\sum_{k_c+1}^{k_u} k^2P(k)\right]. \tag{37}$$

Considering the particular case of an N-node BA model, $P(k) = 2m^2/k^{-3}$, $k_t = m$ and $k_u \doteq mN^{1/2}$, we have from Eq. (37) that

$$\lambda_c^{-1} = m\ln\frac{k_u^{1-a}}{mk_{c+1}^{-a}} = \frac{1}{2}m\ln N - am\ln\frac{mN^{1/2}}{k_{c+1}}. \tag{38}$$

Finally, to calculate the AOS in an infinitely large scale-free network, we have

$$\begin{aligned} R_\infty &= 1 - \sum_k P(k)S_k(\infty) \\ &= 1 - \left(\sum_{k_t}^{k_c}\frac{2m^2}{k^3}\mathrm{e}^{-\lambda k\phi(\infty)} + \sum_{k_{c+1}}^{k_u}\frac{2m^2}{k^3}\mathrm{e}^{-(1-a)\lambda k\phi(\infty)}\right) \\ &= 1 - \left(\int_{k_t}^{\infty}\frac{2m^2}{k^3}\mathrm{e}^{-\lambda k\phi(\infty)}\mathrm{d}k - \int_{k_{c+1}}^{\infty}\frac{2m^2}{k^3}\mathrm{e}^{-\lambda k\phi(\infty)}\mathrm{d}k + \int_{k_{c+1}}^{\infty}\frac{2m^2}{k^3}\mathrm{e}^{-(1-a)\lambda k\phi(\infty)}\mathrm{d}k\right). \end{aligned} \tag{39}$$

Since the integrations in Eq. (39) are in the form of incomplete gamma function, applying Eqs. (17) and (18), we have

$$R_\infty = 2m^2\lambda\phi(\infty)\left(\frac{1}{m} - \frac{a}{k_{c+1}}\right). \tag{40}$$

Also we can derive the expression of $\phi(\infty)$ from Eq. (32) that

$$\begin{aligned} \phi(\infty) &= 1 - \frac{1}{\langle k\rangle}\sum_k kP(k)S_k(\infty) \\ &= 1 - m\left(\int_{k_t}^{\infty} k^{-2}\mathrm{e}^{-\lambda k\phi(\infty)}\mathrm{d}k - \int_{k_{c+1}}^{\infty} k^{-2}\mathrm{e}^{-\lambda k\phi(\infty)}\mathrm{d}k + \int_{k_{c+1}}^{\infty} k^{-2}\mathrm{e}^{-(1-a)\lambda k\phi(\infty)}\mathrm{d}k\right). \end{aligned} \tag{41}$$

Again, the integrations in Eq. (41) can be considered as incomplete gamma functions. Therefore we have the simplified equation of $\phi(\infty)$ that

$$\ln(\phi(\infty)) = \frac{1}{(1-a)\lambda m}\left(-1 + \lambda m\{(1-a)(1-r_E) - \ln m - (1-a)\ln[(1-a)\lambda] - a\ln k_{c+1}\}\right), \tag{42}$$

and consequently,

$$\phi(\infty) = \exp\left[\frac{1}{(1-a)\lambda m}\left(-1 + \lambda m\{(1-a)(1-r_E) - \ln m - (1-a)\ln[(1-a)\lambda] - a\ln k_{c+1}\}\right)\right]. \tag{43}$$

Together with Eq. (39), the network AOS can be calculated. Since a simple closed-form solution of $\phi(\infty)$ is difficult to achieve, we plot figures in Section 4 to demonstrate the respective effects of immunization rate and spreading rate on AOS.

3.3. Partial Link Immunization (PLI)

The mean-field level differential equations for PLI can be presented as:

$$\frac{\mathrm{d}\rho_k(t)}{\mathrm{d}t} = \begin{cases} -\rho_k(t) + (1-a)\lambda k S_k(t)\theta(t) & \text{if } k > k_c\,, \\ -\rho_k(t) + \lambda k S_k(t)\theta(t) & \text{if } k \le k_c\,; \end{cases} \tag{44}$$

$$\frac{\mathrm{d}S_k(t)}{\mathrm{d}t} = \begin{cases} -(1-a)\lambda k S_k(t)\theta(t) & \text{if } k > k_c, \\ -\lambda k S_k(t)\theta(t) & \text{if } k \le k_c; \end{cases} \tag{45}$$

$$\frac{\mathrm{d}R_k(t)}{\mathrm{d}t} = \rho_k(t). \tag{46}$$

Again, the term $(1-a)\lambda k S_k(t)\theta(t)$ in Eqs. (44) and (45) denotes the percentage of k-degree hub nodes that are newly infected at a close-to-threshold spreading rate. Similar to Eqs. (6) and (28) for PNI and PEI respectively, the probability that a randomly selected link is connected to an infected node can be expressed as

$$\theta(t) = \frac{\sum_k kP(k)\rho_k(t)}{\langle k\rangle}. \tag{47}$$

We see that Eqs. (44)–(47) are exactly the same as Eqs. (25)–(28). Therefore, the epidemic threshold and AOS at a spreading rate close to epidemic threshold are the same for PEI and PLI. The AOS of PLI under high spreading rates will be studied by numerical simulations.

3.4. Imperfect targeted immunization in degree-correlated SIR model

To analyze imperfect targeted immunization in the degree-correlated SIR model, the mean-field level equations for PNI can be re-written as follows:

$$\frac{\mathrm{d}\rho_k(t)}{\mathrm{d}t} = -\rho_k(t) + \lambda A(k) k S_k(t)\theta(t); \tag{48}$$

$$\frac{\mathrm{d}S_k(t)}{\mathrm{d}t} = -\lambda A(k) k S_k(t)\theta(t); \tag{49}$$

$$\frac{\mathrm{d}R_k(t)}{\mathrm{d}t} = \rho_k(t). \tag{50}$$

For PEI and PLI, we have

$$\frac{\mathrm{d}\rho_k(t)}{\mathrm{d}t} = \begin{cases} -\rho_k(t) + (1-a)\lambda A(k) k S_k(t)\theta(t) & \text{if } k > k_c, \\ -\rho_k(t) + \lambda A(k) k S_k(t)\theta(t) & \text{if } k \le k_c; \end{cases} \tag{51}$$

$$\frac{\mathrm{d}S_k(t)}{\mathrm{d}t} = \begin{cases} -(1-a)\lambda A(k) k S_k(t)\theta(t) & \text{if } k > k_c, \\ -\lambda A(k) k S_k(t)\theta(t) & \text{if } k \le k_c; \end{cases} \tag{52}$$

$$\frac{\mathrm{d}R_k(t)}{\mathrm{d}t} = \rho_k(t). \tag{53}$$

In all the above equations,

$$\theta(t) = \frac{\sum_k kT(k)P(k)\rho_k(t)}{\langle k\rangle}. \tag{54}$$

Meanwhile, all the initial conditions and assumptions in Sections 3.1–3.3 remain valid. Following the same procedure as that in Sections 3.1–3.3, we can easily derive a general expression of the epidemic threshold that

$$\lambda_c^{-1} = \frac{1}{\langle k\rangle}\left[\sum_{k_t}^{k_u} k^2 P(k)A(k)T(k) - a\sum_{k_c+1}^{k_u} k^2 P(k)A(k)T(k)\right]. \tag{55}$$

Clearly, there still exists a linear relationship between the inverse of the epidemic threshold and the immunization rate. An example case where $A(k) = k^{-\varepsilon}$ and $T(k) = 1$ is illustrated in Fig. 2. Since it is difficult to find a closed-form expression of AOS, numerical results will be presented in the next section.

4. Simulation results and discussions

Numerical simulations have been implemented on a 10,000-node BA model and the AS-level Internet model. For each simulation, a single infected node is randomly selected at the starting point. Following the SIR scheme, the system finally reaches the steady state when all the infected nodes are removed. All the results displayed are averaged from at least 10,000

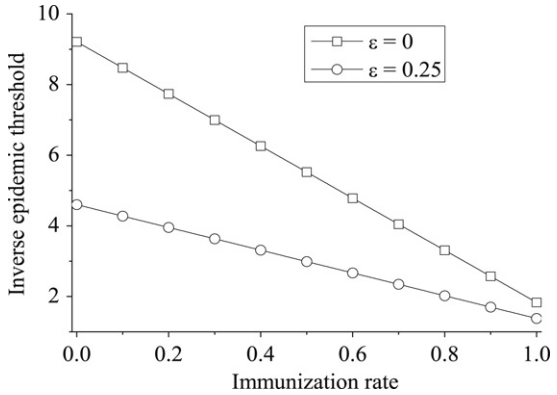

Fig. 2. Dependence of inverse epidemic threshold on immunization rate for correlation functions $A(k) = k^{-\varepsilon}$ and $T(k) = 1$ where $\varepsilon = 0$ and $\varepsilon = 0.25$, respectively, on top of 10,000-node BA model.

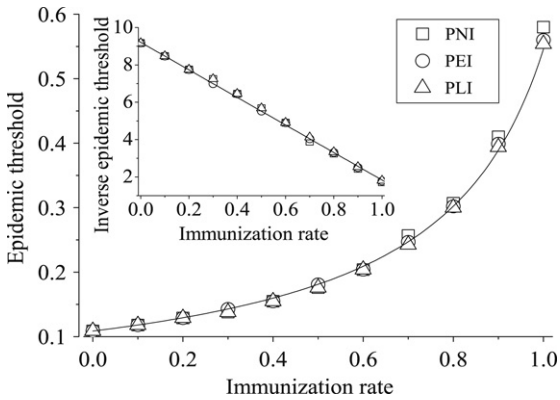

Fig. 3. Dependence of the epidemic threshold on the immunization rate in imperfect targeted immunizations in the BA model. The embedded figure shows the inverse epidemic thresholds. The solid lines in the major and embedded figures show the analytical results.

realizations, each of which with a randomly selected infected node at the starting point. Different realizations may still have the same starting infected node; however, the random process of disease propagation, even under such cases, will not be exactly repeated.

4.1. Epidemic threshold

Simulation results for the BA model are presented in Fig. 3, where we set $k_c = 4$. As we can see, the epidemic threshold increases with the immunization rate a. At the beginning, the increasing speed is slow, and then becomes much faster. With the three different types of imperfect targeted immunizations, the captured epidemic thresholds almost equal to each other. The inverse of the captured epidemic thresholds (i.e., the simulated λ_c^{-1}) versus the corresponding value of a are plotted in the embedded figure. We see that the relationship closely resembles a linear function, which verifies the analytical results.

Simulation results for the AS-level Internet model are presented in Fig. 4. We see that in this correlated network, there is still a roughly linear relationship between the inverse epidemic threshold and the immunization rate. The results suggest that in correlated and uncorrelated large-size scale-free networks, to significantly increase the epidemic threshold, the immunization rate has to be rather high.

4.2. Average Outbreak Size (AOS)

Eqs. (24) and (43) show the relationship between AOS and immunization rate. As in almost all the existing studies, the equations are derived for the case with an infinitely large network size and a close-to-threshold low spreading rate. The analytical results for the case are plotted in Fig. 5 where we set $\lambda = 0.04$ and cut-off $k_c = 4$ for the BA model. Note that the PEI and PLI have the same results. It is clearly shown that even a low immunization rate significantly decreases AOS, although an epidemic outbreak may still happen. Moreover, under a low spreading rate, the AOSs for the three different immunization schemes are almost the same. Under a higher spreading rate, however, different immunization schemes have different impacts on AOS, as illustrated in Fig. 5(b).

To address the changes of AOS in finite-size networks (with or without correlations), numerical simulations have been conducted for 10,000-node BA and AS-level Internet models. The results are presented in Fig. 6, where we set the spreading

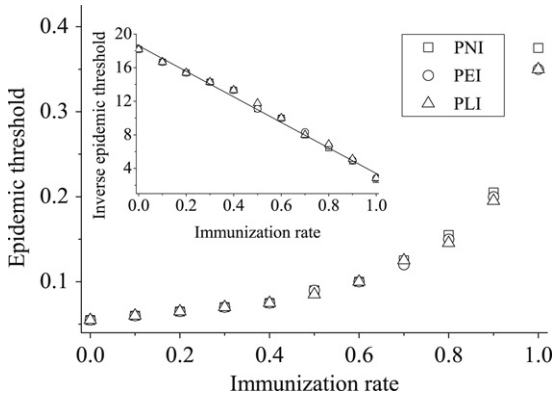

Fig. 4. Dependence of the epidemic threshold on the immunization rate in imperfect targeted immunizations in the AS-level Internet model. The solid line in the embedded figure comes from the least-square linear regression calculations of the captured inverse epidemic thresholds.

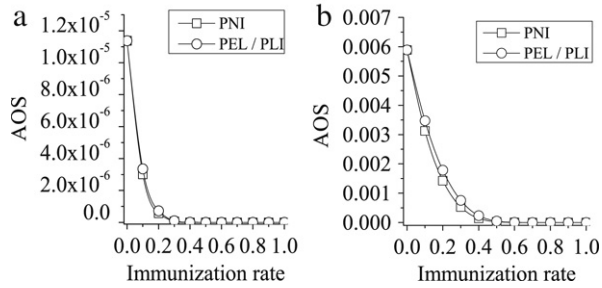

Fig. 5. Analytical results on the dependence of AOS on immunization rate in the infinitely large BA model. The spreading rates are set to be 0.04 and 0.08 for Fig. 5(a) and (b), respectively. Cut-off is set to be 4 for both of them.

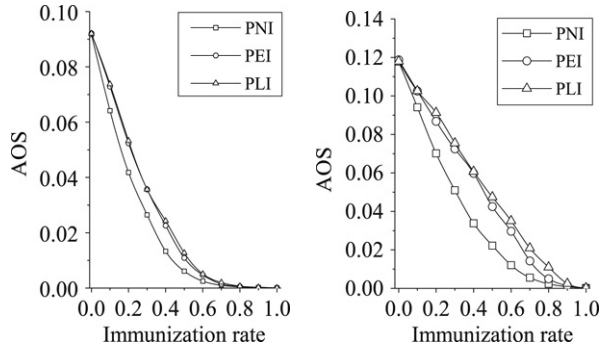

(a) BA model. (b) AS-level Internet model.

Fig. 6. Dependence of AOS on different immunization rates in finite-size networks.

rate and immunization cut-off as 0.25 and 4, respectively. Apparently, a low immunization rate still helps to significantly lower AOS even when the spreading rate is relatively high. Furthermore, we notice that the three imperfect targeted immunizations have different impacts on AOS: PNI and PLI can be viewed as epidemic spreading in scale-free networks with some of their hub nodes and/or links connected to them being removed [36–39]. Compared to PLI, PNI leads to a removal of more hub nodes (a.k.a super-spreader [13,40]) and their links, and consequently a smaller AOS. In PEI, similarly to PNI, some of the hub nodes are protected in each time slot. However, such a protection is not permanent: a node being protected in this time slot can still be affected later on. As a result, PEI leads to a larger AOS than PNI.

4.3. Imperfect targeted immunization in degree-correlated SIR model

To evaluate the performance of imperfect targeted immunization against degree-correlated transmission schemes, as that in Ref. [24] we investigate the special case where $A(k) = k^{-\varepsilon}$ and $T(k) = 1$. A larger value of ε denotes a stronger degree correlation, while $\varepsilon = 0$ reduces to the classic SIR model with no correlation. Fig. 7 illustrates two different cases

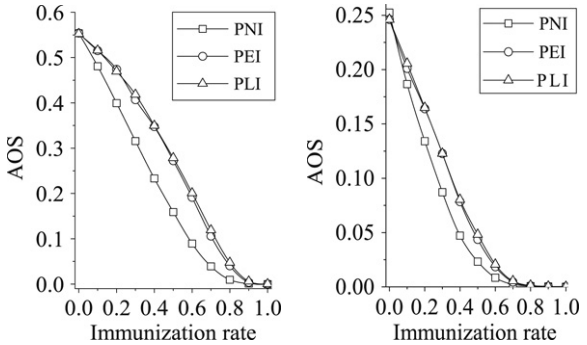

(a) $\varepsilon = 0$. (b) $\varepsilon = 0.25$.

Fig. 7. Dependence of AOS on different immunization rates in BA model with a degree-correlated transmission scheme where $A(k) = k^{-\varepsilon}$ and $T(k) = 1$: (a) $\varepsilon = 0$; and (b) $\varepsilon = 0.25$. Spreading rate and cut-off are set to 0.5 and 4, respectively.

with $\varepsilon = 0$ and $\varepsilon = 0.25$, respectively. We observe that (i) a larger value of ε leads to a smaller AOS; and (ii) for both cases, imperfect targeted immunization remains as effective in reducing AOS even at a moderate immunization rate. Therefore, network robustness is still significantly enhanced.

5. Conclusion

In this paper, we evaluated the effectiveness of imperfect targeted immunization in scale-free networks with classic as well as degree-correlated SIR models. Three different cases have been proposed and analyzed. We found that under the same immunization rate, the three different cases result in the same epidemic threshold but different AOS. A linear relationship between the inverse epidemic threshold and the immunization rate has been identified, which shows that the possibility of having an epidemic outbreak cannot be significantly lowered unless the protection is reasonably strong. On the other hand, even a low immunization rate lowers network AOS significantly.

Our studies have revealed that similar conclusions hold for imperfect targeted immunization on SIS model. Specifically, there exists a linear relationship between the inverse of the epidemic threshold and the immunization rate; meanwhile the number of infections when the system reaches its steady state (termed as prevalence [10]) can be significantly reduced even with a moderate immunization rate. Due to page limit, further details have to be presented in a separate report.

A recent trend in related research is to study complex *adaptive* systems and dynamic networks (e.g., Refs. [41,42]). It is important to realize that many real-life systems will not keep static during epidemic spreading. Understanding the effects of perfect and imperfect targeted immunizations in such systems will be our future research interest.

Acknowledgment

This work is supported in part by the Singapore A*STAR grant BMRC 06/1/21/19/457.

References

[1] A.-L. Barabási, Linked: How Everything is Connected to Everything Else, Plume, 2004.
[2] S. Bornholdt, H.G Schuster (Eds.), Handbook of Graphs and Networks: From the Genome to the Internet, Wiley-VCH, 2003.
[3] M. Faloutsos, P. Faloutsos, C. Faloutsos, SIGCOMM'99 29 (1999) 251.
[4] R. Albert, H. Jeong, A.-L. Barabási, Nature 401 (1999) 130.
[5] H. Jeon, B. Tombor, R. Albert, Z.N. Oltval, A.-L. Barabási, Nature 407 (2000) 651.
[6] R.J. Williams, E.L. Berlow, J.A. Dunne, A.-L. Barabási, N.D. Martinez, Proc. Natl. Acad. Sci. USA 99 (2002) 12913.
[7] D. Garlaschelli, G. Caldarelli, L. Pietronero, Nature 423 (2003) 165.
[8] F. Liljeros, C.R. Edling, L.A.N. Amaral, H.E. Stanley, Y. Aberg, Nature 411 (2001) 907.
[9] S.H. Strogatz, Nature 410 (2001) 268.
[10] R. Pastor-Satorras, A. Vespignani, Phy. Rev. Lett. 86 (2001) 3200.
[11] A.L. Lloyd, R.M. May, Science 292 (2001) 1316.
[12] M.E.J. Newman, Phy. Rev. E 66 (2002) 016128.
[13] Y. Moreno, R. Pastor-Satorras, A. Vespignani, Eur. Phys. J. B 26 (2002) 521.
[14] M. Boguñá, R. Pastor-Satorras, Phy. Rev. E 66 (2002) 047104.
[15] R. Pastor-Satorras, A. Vespignani, Phy. Rev. E 65 (2002) 035108(R).
[16] R. Pastor-Satorras, A. Vespignani, Phy. Rev. E 65 (2002) 036104.
[17] Z. Dezso, A.-L. Barabási, Phy. Rev. E 65 (2002) 055103.
[18] S. Xiao, G. Xiao, T.H. Cheng, IEEE Commun. Mag. 46 (2008) 146.
[19] S. Gandon, M. Mackinnon, S. Nee, A. Read, Proc. R. Soc. Lond. B 270 (2003) 1129.
[20] V.V. Ganusov, R. Antia, Evolution 60 (5) (2006) 957.
[21] P. Yip, R. Watson, Q. Chen, Statist. Med. 26 (2007) 4475.
[22] R.M. Anderson, R.M. May, Infectious Diseases in Humans, Oxford University Press, Oxford, 1992.
[23] J.D. Murray, Mathematical Biology, Springer Verlag, Berlin, 1993.

[24] R. Olinky, L. Stone, Phys. Rev. E 70 (2004) 030902.
[25] M.K. Nordvik, F. Liljeros, Sex. Trans. Dis. 33 (2006) 342–349.
[26] T. Zhou, J.-G. Liu, W.-J. Bai, G. Chen, B.-H. Wang, Phys. Rev. E 74 (2006) 056109.
[27] A.-L. Barabási, R. Albert, Science 286 (1999) 509.
[28] A.-L. Barabási, R. Albert, Rev. Modern Phys. 74 (2002) 47.
[29] http://moat.nlanr.net/Routing/rawdata.
[30] M.E.J. Newman, Phy. Rev. Lett. 89 (2002) 208701.
[31] M. Marder, Phy. Rev. E 75 (2007) 066103.
[32] E. Volz, J. Math. Biol. 56 (3) (2008) 293.
[33] J. Marro, R. Dickman, Nonequilibrium Phase Transitions in Lattice Models, Cambridge University Press, 1999.
[34] S.N. Dorogovtsev, J.F.F. Mendes, Adv. Phys. 51 (2002) 1079.
[35] M. Abramowitz, I. Stegun, Handbook of Mathematical Functions, Dover Pub., New York, 1972.
[36] R. Albert, H. Jeong, A.-L. Barabási, Nature 406 (2000) 378.
[37] S. Martin, R.D. Carr, J.-L. Faulon, Physica A 371 (2006) 870.
[38] P. Holme, B.J. Kim, C.N. Yoon, S.K. Han, Phy. Rev. E 65 (2002) 056109.
[39] A.E. Motter, T. Nishikawa, Y.-C. Lai, Phy. Rev. E 66 (2002) 065103.
[40] R. Fujie, T. Odagaki, Physica A 374 (2007) 843–852.
[41] M.M. Waldrop, Complexity: The Emerging Science at the Edge of Order and Chaos, Simon & Schuster, 1993.
[42] N. Sarshar, V. Roychowdhury, Phy. Rev. E 69 (2004) 026101.